Journal of the European Ceramic Society **19** (1999) 1133–1137

PII: S0955-2219(98)00389-6
0955-2219/99/$ - see front matter

Lead Hafnate Zirconate Titanate-based Perovskite Materials for Actuation

Catherine Heremans[a]*[1] and Harry L. Tuller[b]

[a]PCIM, Université Catholique de Louvain, 1348 Louvain-la-Neuve, Belgium
[b]DMSE, Massachusetts Institute of Technology, Cambridge, MA 02138, USA

Abstract

Antiferroelectric $Pb_{0.98}La_{0.02}(Zr_{0.70}Hf_{0.30})_{1-x}Ti_xO_3$ *(0·065≤x≤0·10) compositions, located close to the boundary with a ferroelectric phase field, have been investigated as potential candidates for actuation through the mechanism of field induced antiferroelectric–ferroelectric phase transition. The materials were analysed by X-ray diffraction and by electromechanical measurements. The compositions with* $x \leq 0{\cdot}075$ *seemed initially located in the orthorhombic (almost tetragonal)* AFE_I *antiferroelectric phase field. They underwent an electrically-induced phase transition into another antiferroelectric* AFE_{II} *phase. Intermediate compositions (*$0{\cdot}0775 \leq x \leq 0{\cdot}095$*) were initially located in the other antiferroelectric phase,* AFE_{II}*, and could be electrically forced in the ferroelectric phase. Remanent ferroelectric behavior at zero field increased from* $x = 0{\cdot}0775$ *to* $x = 0{\cdot}0825$*, until the ferroelectric phase remained metastable for* $0{\cdot}0825 \leq x \leq 0{\cdot}095$*, in analogy with the better studied* $PbNbZrSnTiO_3$ *and* $PbLaZrSnTiO_3$ *systems.* © *1999 Elsevier Science Limited. All rights reserved*

Keywords: X-ray methods, ferroelectric properties, perovskites, PLZT, actuators.

1 Introduction

Actuation through antiferroelectric–ferroelectric phase transition has been demonstrated in PZT,[1] and later extensively in the $PbNbZrSnTiO_3$ and the $PbLaZrSnTiO_3$ systems. These systems present two antiferroelectric phases, AFE_I and AFE_{II} that appear pseudo-tetragonal, but are truly orthorhombic with a commensurate and incommensurate lattice, respectively.[2] The AFE_{II} phase can be electrically forced into a rhombohedrally-distorted ferroelectric phase at fields below the breakdown field, as the free energy difference between the two phases is small. The electric field for phase switching depends on the composition and its distance to the phase boundary with the ferroelectric phase field. The temperature range over which the transition is feasible in turn depends on the slope and sign of the boundary with increasing Ti concentration. In contrast with $PbZrO_3$, $PbHfO_3$ also presents two clearly different pseudo-tetragonal antiferroelectric phases: a low temperature truly orthorhombic phase, AFE_I, and a pseudotetragonal phase (subject of much controversy), AFE_{II}, with a larger unit cell volume and a larger dielectric constant, stable between 163 and 210°C.[3] Phase transitions between both antiferroelectric phases and the ferroelectric phases were reported, but the transition between the two antiferroelectric phases was partially masked by electrical conductivity.[4] In the $Pb(Hf,Ti)O_3$ phase diagram, the phase sequence with increasing temperature for a composition in the FE phase field at room temperature is FE–AFE–PE 1,[5] inverse to that of PZT in the Zr-rich side[1] (see Fig. 1), but analogous to that of the $PbLaZrTiSnO_3$ system with Sn≥20%. An appropriate mixture of the PZT and PHT systems should result in a perfectly morphotropic phase boundary. The ideal ratio of Zr/Hf was determined graphically from the tolerance factor[6] and leads to a precise morphotropic phase boundary composition of $Pb_{0.98}La_{0.02}(Zr_{0.70}Hf_{0.30})_{0.9025}Ti_{0.0975}O_3$. In this work, antiferroelectric compositions of this interesting system were explored for electro-actuation applications (see Fig. 1). As $PbHfO_3$ presents important differences with $PbZrO_3$ new phenomena were expected, which might lead to a better understanding of these complex systems.

*To whom correspondence should be addressed. Fax: +32-1047-4028; e-mail: heremans@pcim.ucl.ac.be
[1]Collaborateur Scientifique, FNRS.

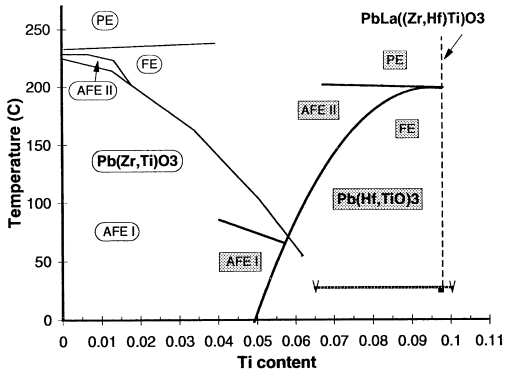

Fig. 1. Phase sequence in the Ti-poor end of the $PbZrTiO_3$ and $PbHfTiO_3$ phase diagram.

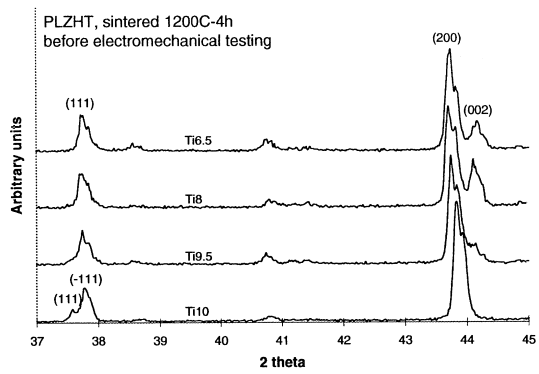

Fig. 2. X-ray diffraction patterns of the sintered samples before electromechanical testing. Pseudotetragonal distortion for Ti6·5, TiS and Ti9·5 with a regular decrease of the splitting of the (200), (002) intensity referenced on the cubic cell and the (111) singlet. Orthorhombic distortion in TAO, with a singlet of (220) and doublet of (111), (−111).

2 Experimental

Ten samples of nominal compositions $Pb_{0.98}La_{0.02}(Zr_{0.70}Hf_{0.30})_{1-x}Ti_xO_3$ with $x = 0.065$, 0·070, 0·075, 0·0775, 0·08, 0·0825, 0·085, 0·0875, 0·090, 0·095 and 0·10 were prepared by conventional solid state reactions and are referred to as Ti6·5 to Ti10. Lead acetate, and the other metal oxides were weighed in appropriate ratios, mixed and ball-milled for 24 h with ethanol. The powders were reground and calcined twice at 850°C for 8 h in a closed crucible, itself contained in a closed container, and protected in a Pb-rich atmosphere supplied by a crucible filled with PZT. The resulting powders were ground and pressed into 1/2 inch diameter pellets at 7 kpsi and isostatically pressed at 40 kpsi. Sintering took place at 1200°C for 4 h in a Pb-rich atmosphere. The sintered samples were analysed by X-ray diffraction using Cu K_α radiation and again after the electromechanical measurements. The longitudinal strain was measured by laser interferometry at 1 Hz using a sinusoidal signal and with a maximum applied voltage of 20 kV. Chemical analysis was performed on the samples after electromechanical testing by wavelength dispersive spectroscopy and showed a slight deficiency in Pb, and a Hf/Zr ratio of 33/67. The Ti content corresponds very well to the nominal compositions.

3 Results and Discussion

3.1 X-rays

In the patterns of the sintered samples shown in Fig. 2, the perovskite intensities refer to a metrically tetragonal structure before electromechanical testing up to Ti9·5. It is however impossible to conclusively assign a tetragonal structure to these samples on the basis of X-ray powder diffraction, as commensurate and/or incommensurate superstructures, known to play a major role in samples of this nature, are not detectable by these means.[2,7,8] The X-ray pattern of Ti10 refers to a strictly rhombohedral unit cell, representative of an initially ferroelectric phase. After electromechanical testing, the patterns of Ti8·25 to Ti8·75 (not shown) clearly indicate a mixture between the tetragonal and the rhombohedral distortion of the unit cell, although the samples were originally in the tetragonal phase field.

3.2 Electromechanical

In Ti6·5 (not shown), only a small amount of electrostrictive behavior is observed, with a linear P–E dependence. The P–E and strain–E curves of Ti are shown in Figs 3(a) and 4(a). Beyond $E_{c1} = 7{\cdot}1\ \mathrm{kV\,mm^{-1}}$, the polarisation, which behaved linearly to that point, exhibits a sudden increase that occurs upon subsequent cycling at a critical field E_c of $1\ \mathrm{kV\,mm^{-1}}$. This marks a transition to a new phase, in which the P–E dependence is again linear, but with a higher dielectric constant. These two features are consistent with a transition between the AFE_I and AFE_{II} antiferroelectric phases.[1,3,6] Up to the initial critical field E_{c1}, a typical quadratic electrostrictive strain behavior with field is observed. Beyond E_{c1}, the longitudinal strain loops are clearly not of the same nature as the typical double loops of an antiferroelectric–ferroelectric phase transition. For $E \geq E_c$, the strain increases regularly by electrostriction in the AFE_{II} phase. Saturation, typically expected for a ferroelectric phase, is not reached. On reducing the field, the strain decreases with a limited amount of hysteresis.

In Ti7·5, the behavior in both the initial AFE_I and the induced AFE_{II} phase are comparable to those in Ti7. E_{c1} and E_c amount, respectively, to 4·7 and again $1\ \mathrm{kV\,mm^{-1}}$, as in Ti7. This sample, however, shows signs of FE behavior at higher fields with increased hysteresis. This situation was previously described in high La-containing $PbLaZrTiO_3$ ceramics.[9] The material can be poled

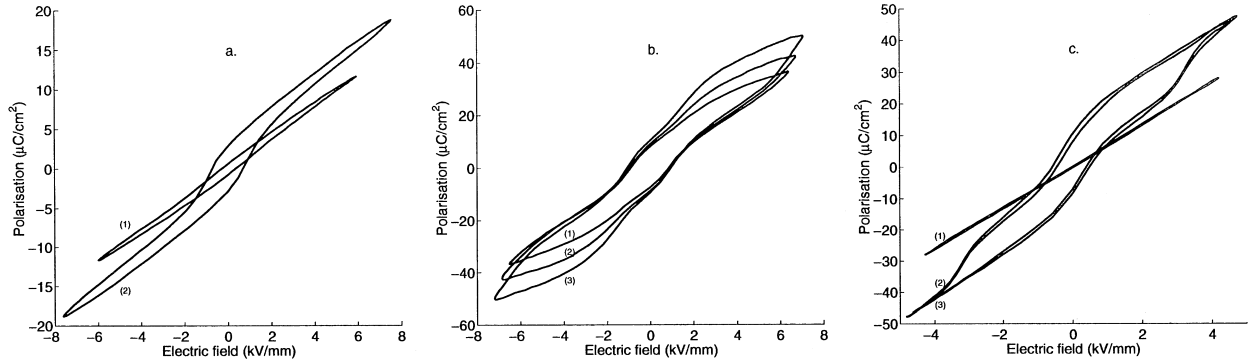

Fig. 3. P versus E at room temperature with increasing applied fields: (a) Ti7; (b) $x = 0{\cdot}07$ sintered at 1250°C; (c) Ti 7·75.

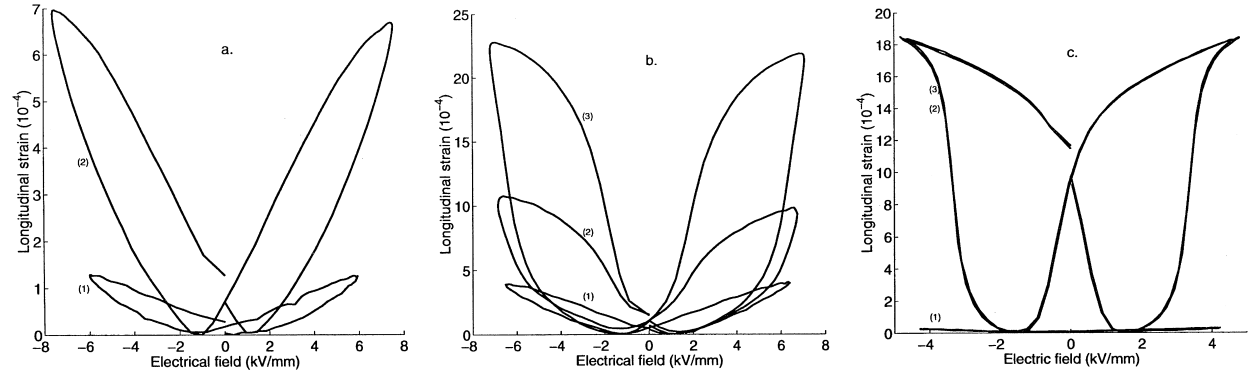

Fig. 4. Strain versus E at room temperature with increasing applied fields: (a) Ti7; (b) $x = 0{\cdot}07$ sintered at 1250°C; (c) Ti7·75.

to a FE-like level but lacks stable remanence. There is however some indication of a transition around $5{\cdot}5\,\mathrm{kV\,mm^{-1}}$ into a true ferroelectric phase. A better illustration of this sequence occurs in a sample of a slightly lower nominal Ti content ($x = 0{\cdot}07$) but sintered at 1250°C, as shown in Figs 3(b) and 4(b). The higher sintering temperature could result in a higher experimental Ti content by increased Pb loss from the sample. It exhibits the same characteristics as Ti7·5 up to $5\,\mathrm{kV\,mm^{-1}}$, i.e. AFE_I–AFE_{II} switching with a stepwise increase of P at $E_c = 1\,\mathrm{kV\,mm^{-1}}$. At higher fields, another important increase of the strain and the polarisation occurs subsequently around $E_F = 5{\cdot}3\,\mathrm{kV\,mm^{-1}}$, indicative of a real phase transition into the ferroelectric phase. Neither E_C, nor E_F are dependent on the total applied field.

The electrically-forced AFE_I–AFE_{II} transition and, a fortiori, the multiple switching events, AFE_I–AFE_{II}-FE described above are rarely reported in the literature in contrast with the analogous thermally and compositionally-induced transitions. They have been suggested on single crystal platelets of $PbHfO_3$, but the first transition had not been clearly detected because of the electrical conductivity of the samples.[4] In the present PLHZT system, La increases the resistivity and might therefore provide better evidence of this electrically induced transition. Moreover, the low value of E_C ($1\,\mathrm{kV\,mm^{-1}}$) is incompatible with a transition between the antiferroelectric and the ferroelectric phases for compositions so remote from the phase boundary. The values of E_F ($5\,\mathrm{kV\,mm^{-1}}$) for AFE_{II}–FE reported here are in the expected range. On single crystal platelets of $PbHfO_3$ values of 7 and $15\,\mathrm{kV\,mm^{-1}}$ were reported for the AFE_I–AFE_{II} and the AFE_{II}–FE transitions, respectively.[4] The much lower values in the present materials could be partly attributed to the presence of Ti, which stabilises the AFE_{II} and the FE phases.[5] The increase of the strain with field in both antiferroelectric phases is electrostrictive in nature and does not saturate at high fields. The electrostrictive coefficients appear different between the two antiferroelectric phases as they depend among other things on the coupling between the two sublattice polarisations.[10] The electrostriction might also mask the slight intrinsic volume expansion between AFE_I and AFE_{II}.

Ti7·75 (shown in Figs 3(c) and 4(c)) and Ti8 are initially antiferroelectric (AFE_{II}). P behaves linearly with E at low fields and the strain curve indicates a very limited degree of electrostriction. Beyond the initial critical field $E_{F1} = 4{\cdot}5\,\mathrm{kV\,mm^{-1}}$ for Ti7·75, the ceramic is forced into the ferroelectric phase, obeying a well-defined double loop behavior with no appearance of quadruple loop. Remanent strain is present at zero field due to some ferroelectric phase. The subsequent switching field, E_F, decreases to $3\,\mathrm{kV\,mm^{-1}}$, a typical value

for the field-forced transition between the AFE_{II} and the FE phases. E_F is not a function of the applied electrical fields for $E \geq E_{F1}$, in agreement with the thermodynamic reversibility model of Yang and Payne.[11] The remanent ferroelectricity at zero field increases with x and indicates a decrease of the strength of the antiferroelectric sublattice coupling. Well-defined AFE_{II}–FE double loops with zero remanent strain at zero field would typically emerge at lower x, deeper in the AFE_{II} phase field. They are however not observed in this system as the AFE_I phase field is hit first on decreasing x. A more detailed study of the temperature dependence of the compositions in the present system will be dealt with in another paper.

From Ti8·25 to Ti9·5, the material switches directly from the AFE_{II} phase into a metastable ferroelectric phase with typical ferroelectric strain and polarisation loops. The coercive field of the metastable phase systematically ranges around $1\,kV\,mm^{-1}$, although the initial switching fields E_{F1}, all larger than $1\,kV\,mm^{-1}$, decrease with x. Yet, X-rays showed that the compositions retain a distinct pseudotetragonal character from the structural standpoint. The amount of tetragonal character retained after switching decreases on approaching the phase boundary.

Ti10, the only sample theoretically located in the ferroelectric phase field exhibits a dielectric and strain curves typical of a ferroelectric with a coercive field of $1\,kV\,mm^{-1}$, in perfect corroboration with the structural data.

4 General Phase Diagram

The phase diagram of the PLZHT system presents two phase boundaries with increasing x, as summarized in Fig. 5. The first boundary, between AFE_I and AFE_{II}, is located around $x = 0{\cdot}075$ and $0{\cdot}0775$. The second one, between AFE_{II} and FE was detected in the present work between $x = 0{\cdot}095$ and $x = 0{\cdot}10$ by X-ray diffraction, a non disruptive tool for materials that are sensitive to electromechanical effects.[5] This is in excellent agreement with the theoretical boundary at $x = 0{\cdot}0975$.[6] The X-ray method is not powerful enough for detecting the slight differences between the two antiferroelectric phases as their main signature in an X-ray diffraction pattern is the presence of weak superstructure intensifies.[2] Many different types of antiferroelectric behavior are however detectable electromechanically, from intrinsic AFE_I and AFE_{II} for Ti6·5 and Ti7·75, respectively, to a more intricate behavior for intermediate compositions. In particular, electrostriction in the AFE_{II} phase seems to be more important in materials induced in this phase from AFE_I than in the initially AFE_{II} materials. In the induced case, local inhomogeneities could possibly be created in the lattice, favor the formation of polar nanodomains in the antiferroelectric matrix and promote electrostriction. The complexity of the many different antiferroelectric orderings reminds one of the PLZT system[7,8] and only a detailed microscopy work can resolve many of the unanswered questions. The existence of intermediate orderings in the PLZT system resulted from the presence of La. This aliovalent substituant creates vacancies and breaks up the long range ferroelectric order, thereby favoring either the nanodomain state as in relaxors, or incommensuration as in antiferroelectrics. Similar complexity is easily conceivable in the present Hf-containing systems. Hf, although isovalent with Zr and Ti, widens the AFE_{II} phase stability range, and also possibly plays a role in incommensuration. The larger differences in volume expansion and dielectric constant between AFE_I and AFE_{II} of $PbHfO_3$ makes the $PbLaZrHfTiO_3$ system an excellent candidate to analyse fundamental phenomena related to antiferroelectric phase fields and phase transitions.

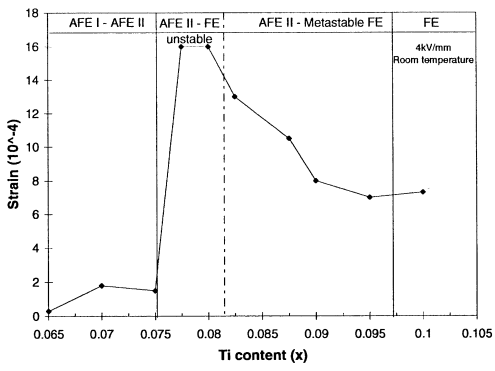

Fig. 5. Electrically-induced strain as a function of Ti content at room temperature for the Ti6·5 to Ti10 series at $4\,kV\,mm^{-1}$.

Acknowledgements

This research was sponsored by the ARO under contract DAAH04-95-1-0104. The first author gratefully acknowledges the financial support of the Fonds National de la Recherche Scientifique, Belgium. The authors are very grateful to Professor N. Hagood and Professor Y. M. Chiang for useful discussions and S. Wordsworth and P. Trappa for technical assistance.

References

1. Sawaguchi, E., Ferroelectricity versus antiferroelectricity in the solid solutions of $PbZrO_3$ and $PbTiO_3$. *J. Phys. Soc. Japan*, 1953, **8**(5), 615–629.

2. Speck, J. S., De Graef, M., Wilkinson, A. P., Cheetham, A. K. and Clarke, D. R., Hierarchical domain structures and in situ domain migration in the antiferroelectric ceramic PLSnZT. *J. Appl. Phys.*, 1993, **73**, 7261–7267.
3. Shirane, G. and Pepinsky, R., Phase transitions in antiferroelectric $PbHfO_3$. *Physical Review*, 1953, **91**(4), 812–815.
4. Fesenko, O. E. and Balyunis, L. E., The temperature–electric field phase diagram of lead hafnate. *Ferroelectrics*, 1980, **29**, 95–98.
5. Hall, C. A., Dungan, R. H. and Stark, A. H., Solid solutions in the antiferroelectric region of the system $PbHfO_3$–$PbTiO_3$–$PbSnO_3$–$PbNb_2O_6$. *J. Am. Ceram. Soc.*, 1964, **47**(6), 259–264.
6. Grange, G., Perlourson, A. and Troccaz, M., Céramiques ferroélectriques à faible pression de transition ferroélectrique–antiferroélectrique. *C. R. Acad. Sc. Paris*, 1982, **294**(Serie II), 1123–1126.
7. Dai, X., Xu, Z., Li, J-.F. and Viehland, D., Effects of lanthanum modification on rhombohedral $Pb(Zr_{1-x}Ti_x)O_3$ ceramics: part 1. Transformation from normal to relaxor ferroelectric behaviors. *J. Mater. Res.*, 1996, **11**(3), 618–625.
8. Dai, X., Xu, Z., Li, J.-F. and Viehland, D., Effects of lanthanum modification on rhombohedral $Pb(Zr_{1-x}Ti_xO_3$ ceramics: part Il. Relaxor behavior versus enhanced antiferroelectric stability. *J. Mater. Res.*, 1996, **11**(3), 626–638.
9. Meng, Z. Y., Kumar, U. and Cross, L. E., Electrostriction in lead lanthanum zirconate–titanate ceramics. *J. Am. Ceram. Soc.*, 1985, **68**(8), 459–462.
10. Uchino, K., Cross, L. E., Newnham, R. and Nomura, S., Electrostrictive effects in antiferroelectric perovskites. *J. Appl. Phys.*, 1981, **52**(3), 1455–1459.
11. Yang, P. and Payne, D. A., Thermal stability of field-forced and field-assisted antiferroelectric–ferroelectric phase transformations in $Pb(Zr,Sn,Ti)O_3$. *J. Appl. Phys.*, 1992, **71**(3), 1361–1367.